Available online at www.sciencedirect.com

ScienceDirect

Procedia Structural Integrity 18 (2019) 781–791

Structural Integrity Procedia

www.elsevier.com/locate/procedia

25th International Conference on Fracture and Structural Integrity

Fatigue damage analysis of composite materials using thermography-based techniques

R. De Finis[a]*, D. Palumbo[a], U. Galietti[a]

[a]*Department of Mechanics, Mathematics and Management (DMMM) Politecnico di Bari-Viale Japigia 182, Bari 70126-Italy*

Abstract

Composite materials are nowadays used in many fields of industry, especially for producing large structural components in many applications ranging from naval to aerospace.
Beside to the capability and versatility of uses, the study of damage in composites is not easy due to the different failure mechanisms that can occur simultaneously or in different conditions. The characterisation of composites represents then a critical stage of assessing mechanical properties and resistance and a careful attention has to be put in the study and damage analysis. Due to this, the fatigue performances imposed by Standards have to be verified by means of experimental techniques involving experimental campaign in laboratory on samples or directly on large components. However, classical procedures for evaluating the fatigue resistance of materials present two issues: the expensive and time-consuming tests because of the high number of specimens being tested, and the totally absence of information on occurring damage. In the last few years, great efforts have been made to develop a number of methods aimed at reducing testing time and, subsequently, the cost of the experimental campaign. Among the different techniques, for instance, thermographic methods are considered as a useful tool for the rapid evaluation of fatigue damage and fatigue resistance at specific cycles number (endurance limit).
The capability of thermography, is not only, related to the experimental procedure providing specific tests capable of assessing fatigue resistance in accelerated way, but also to study the energy involved in the fatigue processes.
As previously said, damage mechanisms in composite materials are difficult to be understood and even a small scale anomaly can lead the failure of the material without visible damage or visible signs of the onset of failure phenomena. For this reason, energy intrinsically dissipated can be another point of view to face up to a sudden failure. In this way, energy-related parameters assessed by the analysis of thermographic signal can be useful for assessing information related to the onset of irreversible damage.
The focus of the present research is to provide an innovative method for process thermal signal from innovative composites obtained by Automated Fiber Placement process in order to understand the fatigue behaviour qualitatively and quantitatively.

Peer-review under responsibility of the Gruppo Italiano Frattura (IGF) ExCo.

* Corresponding author.
E-mail address: rosa.definis@poliba.it

2452-3216
Peer-review under responsibility of the Gruppo Italiano Frattura (IGF) ExCo.
10.1016/j.prostr.2019.08.227

Keywords: CFRP composites; Automated Fiber Placement technology; Fatigue process; Damage analysis; Thermal signal analysis; Thermoelastic Stress Analysis

1. Introduction

Composites materials show high performance requirement in different industrial fields such as boating-yachting, aeronautical or aerospace industry Bannister (2004) and wind turbine blades due to high specific stiffness, strength, and good mechanical behavior Palumbo (2016), however, it is very well-known that the fatigue characterisation using standard test method is expensive and time consuming Harris (2003).

In order to reduce test time and costs of fatigue tests, several methods have been proposed to study rapidly and consistently the various damage phenomena, Munoz (2016), Goidescu (2013), Naderi(2012), Kordatos (2012).

The potentialities of thermography to fatigue characterize the composites are exploited by the Thermoelastic Stress Analysis (TSA). The well-known technique is a non-contact, full field technique that provides stress maps of a component subjected to dynamic loading Harwood (1991), Pittaresi (1999), Wang(2010), Palumbo (2016). The theoretical framework refers to the thermoelastic effect arising from cyclic loading applied to a component.

Emery (2010) discussed the benefit of using TSA on composites by investigating different stacking sequences of polymer-matrix-composites. In particular, the stiffness degradation and strain redistributions in between lamina or composite regions where opportunely analysed compared to different thermoelastic metrics.

The use of thermoelastic phase signal was discussed by Fruehmann (2010), in order to detect fatigue damage at low stress amplitude.

The exigence of an in-depth study of the damage (stiffness degradation, failure mechanisms) of fundamental importance to characterize the behaviour of complex shaped components such as those adopted as structural parts components.

In fact, advanced aircraft structures, nowadays contain high percentage by weight of composite components. This allows producing large dimension components in small-time as the production rate forces composite structure producers finding more cost efficient manufacturing methods Denkena(2016), Aized(2011), Kozaczu(2016), Brüning(2017), Belhaj(2013), Zhao(2018).

To reduce, hence, the time to market of composite innovative components, during the last decades, Automated Fiber Placement (AFP) technology was proposed and developed becoming more and more popular and affordable. Today, AFP process is used several aero-structure manufactures which successfully incorporated and certified this method for their products Belnoue(2017), Schmidt (2016), Lichtinger(2015).

In this work, the fatigue behavior of quasi-isotropic CFRP obtained by AFP process was studied and the mechanical degradation of the material is discussed in terms of significant temperature variations. To do this, the adopted processing procedure is presented Krapez (2000), capable of providing thermoelastic signal.

The thermoelastic signal, in fact, can support the understanding and study of the stiffness degradation and strain/stress distribution/redistribution in between lamina.

The strong point of the proposed method is such that thermoelstic signal leads to obtain quantitatively and qualitatively the failure areas, a significant reference in performing non-destructing inspections.

2. Theoretical field

During dynamic loading two thermal effects are generated: thermoelastic heat sources and intrinsic dissipations. The first represents the well-known thermoelastic coupling term related to dynamic loading while, intrinsic dissipation is thermodynamically irreversible. Dissipative phenomena arise due to the viscoelasto-plastic nature of the matrix material, matrix cracking, fibre fracture, and interface cracking /friction among others Montesano(2013), De Finis(2019), Palumbo(2017), Pierron (2007).

Whether the adiabatic conditions are achieved, the temperature changes ΔTel for orthotropic materials are related to the changes in the stresses in the material principal directions by the following expression:

$$\Delta T_{el} = -\frac{T_0}{\rho C_p}\left(\alpha_1 \Delta\sigma_1 + \alpha_2 \Delta\sigma_2\right) \tag{1}$$

where α_1 and α_2 are, respectively the coefficients of linear thermal expansion relative to the principal axes, C_p is the specific heat at constant pressure, ρ is the density, T_0 is the absolute temperature and $\Delta\sigma_1$ and $\Delta\sigma_2$ are the principal stresses.

Typical TSA acquisition systems provide usually a not radiometrically calibrated S signal proportional to the peak-to-peak variation in temperature during the cyclical variation of the sum of principal stress. Usually the signal S is presented as a vector, where modulus is proportional to the change in temperature due to the thermoelastic effect and the phase φ means the angular shift between the thermoelastic and the reference signal provided by loading machine Montesano (2013). In this case, the following equation can be used:

$$A^* S = \left(\alpha_1 \Delta\sigma_1 + \alpha_2 \Delta\sigma_2\right) \tag{2}$$

where A is a calibration constant. In time domain, the equation (2) can be expressed as follows:

$$s = \frac{S}{2}\sin(\omega t + \pi + \varphi) \tag{3}$$

where s is the uncalibrated thermographic signal, ω is the angular velocity and φ is the phase angle between temperature and loading signal. The phase angle remains locally constant in presence of linear elastic behaviour of material and thus, if adiabatic conditions are achieved. If damage occurs non-linearity of thermoelastic signal and phase variations can be observed, Fruehmann (2010).

Intrinsic dissipations are irreversible sources opposed to thermoelastic ones. The presence of irreversible phenomena affects temperature by determining both an increase of mean temperature of the specimen and the occurrence of second order temperature variations. In following paragraph, it will be presented the algorithm to obtain these indexes from temperature signal.

Fig. 1. Coriolis ® robotic system equipped with a roller of the Robotic system, Denkena (2016).

3. Experimental campaign and data processing

Before presenting the tested material a brief introduction about the process is provided. Automatic Fiber Placement technology is aimed to lay composite layer (0,25” width) as unidirectional prepreg tapes, Belnoue(2017), Schmidt (2016), Lichtinger(2015). Each tape is laid down by a robotic system with butt joint in any orientation: this clearly

represents the advantage of producing isotropic structures capable to carry load in any direction. Each tape is pressed to the mould by a roller for proper compaction which is installed on robotic arm (Fig. 1).
The tested material was CFRP panel (fifteen plies of an epoxy-type resin reinforced by carbon fibers with a stacking sequence of [0/-45/45/90/90/45/-45/0]2), from which specimens were extracted. The global panel was 560 mm (weight) and 695 mm (length), samples extracted was designed according to the Standard ASTM D3039. The dimension of specimens were: 25 mm width, 250 mm length and thickness of 3.5 mm. All the specimens were tested on a INSTROM 8850 (250 kN capacity) servo-hydraulic machine.
Nine samples were tested with conventional constant amplitude procedure, in load control, in order to obtain the S-N curve conducted at stress ratio of 0.1 and a loading frequency of 7 Hz, runout 2*10^6 cycles. The imposed loading level of SN curve were compared to ultimate tensile strength (UTS) of the material which is 827 MPa, previously evaluated. The imposed stress levels were six: 50 UTS% (maximum stress: 413.5 MPa), 60% UTS (maximum stress: 496 MPa), 65%UTS (maximum stress: 537.5 MPa), 70%UTS (maximum stress: 579 MPa), 75% UTS (maximum stress: 620 MPa), 80%UTS (maximum stress: 661 MPa).

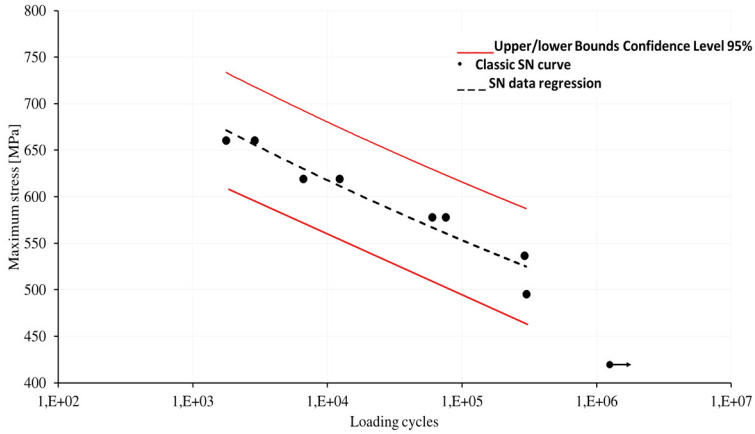

(a)

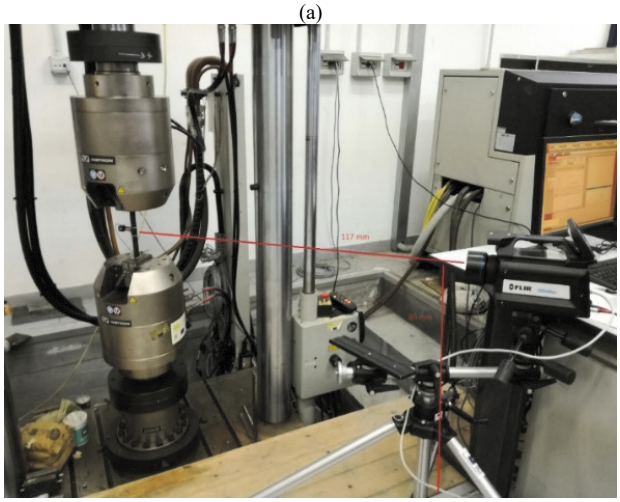

(b)

Fig. 2. Obtained SN curve (a), Layout of loading frame and infrared camera (b).

Fig. 2 reports the experimental SN curve for material (a) and the set-up (b). The equipment involves also an extensometer with the purpose of acquiring strain and stress cycles per cycles. This leads to calculating the global secant Young's modulus for specimens. The evaluation of Young modulus was to provide a metric with which to compare the thermoelastic signal data by fixing the residual stiffness of the specimens after cycles.
The SN curve reported in Fig. 2a shows as the endurance limit is present in correspondence of 50%UTS at 412.5 MPa in terms of maximum stress. All the data lies in the 95% confidence bounds. In Fig. 2a, is represented the loading

frame, and the infrared detector used for thermographic acquisition which was positioned in from of the gage length of the sample.
The IR camera provided a cooled In-Sb detector FLIR X6540 SC (640X512 pixel matrix array, with thermal sensitivity NETD < 30 mK). FLIR X6540 SC acquired at fixed time instant of the tests. The adopted acquisition frequency was 177 Hz. The analysis of thermoelastic signal involved three stress levels: 50% UTS, 65% UTS and 70%UTS respectively at 413.5 MPa, 537.5 MPa, 579 MPa of maximum stresses. The endurance limit obtained was in correspondence of 50%UTS at 413 MPa.
Thermal sequences were processed using specific algorithms providing a thermal signal reconstruction De Finis (2019). The algorithms finally provides pixel by pixel information about the temperature of the specimen 'Sm'. As reported in equation (4) 'Sm' is decomposed in:

$$S_m(t) = S_0 + at + S1\sin(\omega t + \varphi) + S2\sin(2\omega t) \quad (4)$$

the contribution *'S0 + at '* of the mean temperature increase during the cyclic mechanical loading, 'ω' the angular frequency of the mechanical imposed load, *'S1' and 'φ'* respectively the amplitude and phase of first harmonic component of Fourier series while, *'S2'* the amplitude of the second Fourier harmonic component. In particular, the harmonic term *'S1/ S0'* related to thermoelastic temperature signal variation normalised to mean temperature signal is object of the present investigation.
The *'S2'* term is proportional to the amplitude of intrinsic dissipations. In this paper, as previously said, the *'S1/ S0'* term was considered for the analysis referring to 95° and 5° percentile values extracted from the maps, this for firstly avoiding any outlier data point and secondly for taking into account both the phenomena related to stiffness degradation and stress/strain redistribution in through the lamina as explained by Emery(2010). The values of thermoelastic temperature signal variations are referred to the value of an undamaged condition.

4. Results

The constant amplitude tests, as previously shown, were thermographic monitored in order to assess the thermal signal. Firstly, thermoelastic temperature signal normalised per mean temperature was obtained and studied. The thermoelastic temperature signal variations as found by Wang(2010), Krapez(2000), are related to the thermoelastic energy of material which is low at low stress amplitudes and increases as the degradation of the mechanical properties occurs. Specifically for the longitudinal modulus of the material, as the material elastic properties reduce the load imposed reduces as the stiffness reduces12. However, it is difficult to determine quantitatively this energy, especially due to complex damage mechanisms involved in fatigue and due to the brittle behaviour of material.

In Fig. 3 the results of the calculation of Young modulus at each stress level imposed during the classic constant-amplitude tests are reported for three samples: from the one tested at 50%UTS through sample tested at 65%UTS to the one tested at 70%UTS. The values of Young modulus have been related to the value of Young modulus of virgin sample, which practically corresponds to the elastic modulus calculated at initial stages of the test. The markers on each curve of Fig. 3 corresponds to the cycles at which elastic modulus calculations have been made, hence each curve represents a data fitting. According to the literature Huanga(2019), in general, the stiffness of the composites reduces thought the cycles as effect of occurring damage. The entity of the variation depends on the load Ospina Cadavid (2017) and in general an initial stage of stabilisation is recorded which lasts few cycles compared to the total duration of the tests. This initial stage is governed by micro-cracks initiation phenomena and is very short as the load increases. The second stage is governed by the delamination or cracks occurring in the matrix, this phase is slow and occurs with steady growth of damage processes. The third stage is a dramatic elastic properties reduction coupled with final failure of the material. This latter stage lasts few cycles.

The long-lasting stage one is the second stage with a quasi-stable damage growth rate accounting for the most parts of the total cycle numbers.

The behaviour presented in Fig. 3, is in agreement with the theoretical behaviour, in particular, for this quasi-isotropic composite produced by AFP process, the lower are the stresses the more the initial phase lasts. The same as for the second stage: obviously, the lower the stresses are, the more this phase lasts.

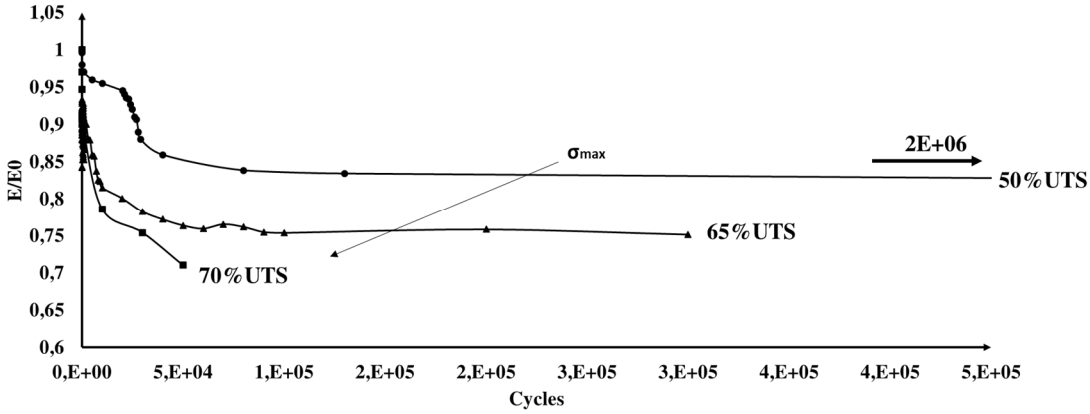

Fig. 3. Stiffness degradation cycle after cycle during constant amplitude test at different imposed loads.

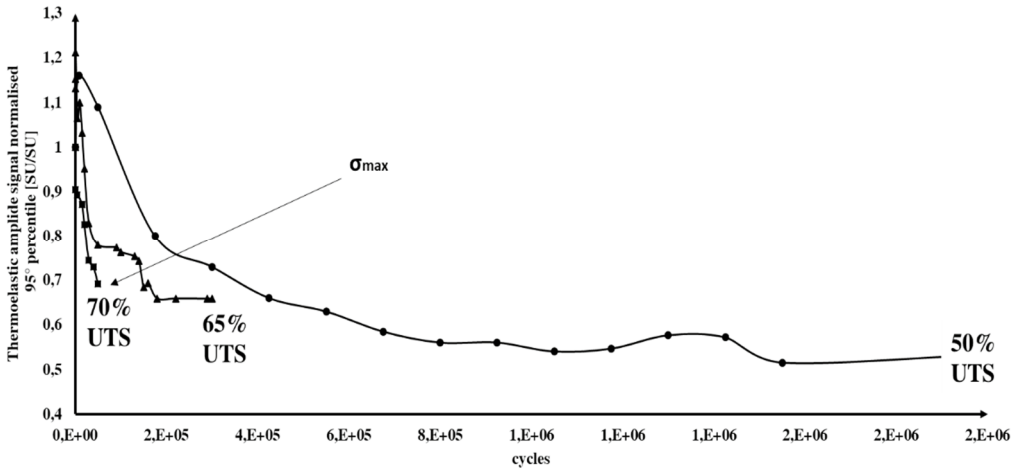

(a)

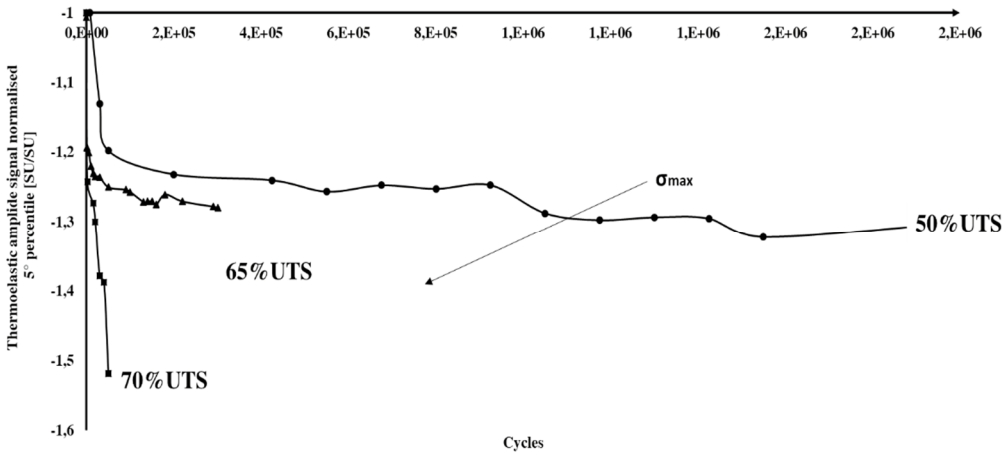

(b)

Fig. 4. Thermoelastic signal variations: (a) 95° and (b)5° percentile values at three stress level of constant amplitude testsStiffness degradation cycle after cycle during constant amplitude test at different imposed loads.

The mechanical data have been compared with thermal data represented by thermoelastic uncalibrated signal variations. The values considered for the analysis of the thermoelastic signal were the maximum value represented by 95° percentile and the minimum represented by 5° percentile related to mean temperature. Those signal variations are strictly correlated to the sum of the changes in the principal stresses Wang (2010), Emery (2010), Fruhemann (2010). The thermal signal maps have been also referred to undamaged/unload condition represented by the thermoealstic values at initial loading level. This clearly emphasizes the different temperature variations which are characterized by higher or lower thermoelastic signal.

In particular, the lower thermoelastic signal variations are correlated to the reduction in stress or strain in certain areas as the load carrying capacity reduces (and the stiffness degradates). The higher values are related to the capability to redistribute stress or strain redistribution as the damage increases.

In Fig. 4, are reported the curves of higher/lower values of thermoelastic signal. The lower values of the 5° percentile are negative in values since, as previously explained they are referred to undamaged condition.

In Fig. 4(a) the values of 95° percentile of thermoelastic signal decreases after an initial increase which has been blurred by a flattened scale for y-axis.

In further graph the same values will be reported coupled with the Young modulus reduction for a specific imposed stress level.

Fig. 4(b) reports the graphs of negative values of thermoealstic signal that refers to 5° percentile values, in these graphs after the initial higher values, one can observe a significant increase in terms of negative values.

Referring to all the samples the entity of 'decrease' of thermal indexes at the end of the test is more severe than the decrease in the stiffness (referred to E/E0 metrics). These finding demonstrates a higher sensitivity of the thermal indexes to record even small variations in the mechanical behaviour of the material.

In Fig. 5 are represented the data in terms of maximum/minimum values of thermoelastic temperature signal variation for each test compared to the mechanical parameter E/E0 representing the stiffness degradation of the material.

In Fig. 5(a-c-e) are reported for each test the 5° percentile values. In the graphs, after the first maximum value, the trend is generally decreasing. The thermoelastic metric 5° percentile exhibits a severe slope variation in those cycles, immediately after the begin of the test.

The thermal analysis made by using the thermoelastic parameters is more sensitive to properties reductions than the one made by using the extensometer data. In fact, the related data are averaged in the gauge length of the sample. So, to use thermal data allows performing a more local and conservative determination of both the time and the location where the mechanical properties degrade.

In Fig. 5(b-d-f) are reported the trend for 95° percentile, the second metrics evaluated. The trend of this parameter is more complex since after an initial increase (which is clearly detectable especially for lower stress levels) an immediate decrease follows. However, after the first decrease which occurs roughly at 10^2-10^3 cycles there is another less pronounced decrease before the failure.

A possible explanation of these results can be in part attributed to the mismatch in the Poisson's ratio between the different lamina of the composite which induces interlaminar shear that determines strain values capable of causing cracks in the matrix. Such the matrix stress/strain concentration increases up to a saturation point, at fixed stress, and the stress can be redistributed at local level into the sound, that are the unbroken parts of the samples. This can explain the slight stabilisation of both 95° and 5° at 50%UTS and 65%UTS. This means that the stress is moving to the adjacent plies. The delamination results in a reduction in the capability of carry out stress/strain concentration at local level. In the case of quasi-isotropic stacking sequence, the stiffness reduction can be attributed to crack occurring at intermediate level plies.

Another strong point of the adopted technique is represented by the possibility to assess where and when damage and failure occur. To do this,-thermoelastic maps are reported for the three tests in Fig. 6. As previously said, the analysis of thermoelastic temperature signal variations leads to localize the damaged areas of material, as the thermoelastic signal variations are related to the redistribution of the stresses caused by the stiffness degradation due to the damage, Fig. 6.

As is possible to see in Fig. 6 at each stress level imposed, there is the effect of the signal of fibres oriented at 90° with respect to the loading direction. This signal appear at each stress level and it seems to be related to intrinsic phenomena occurring between the layers. By observing the images in Fig. 6 it is possible to see intense delamination phenomena. This reflects what found quantitatively by analysing both thermal and mechanical data where the second

stage in the stiffness degradation stage not only is long-lasting but also is characterized by a stabilization of the properties as also observed by the 5° percentile of thermoelastic data. In the same area where the maximum negative value is achieved in terms of thermal metrics the delamination occur (Fig. 6a).

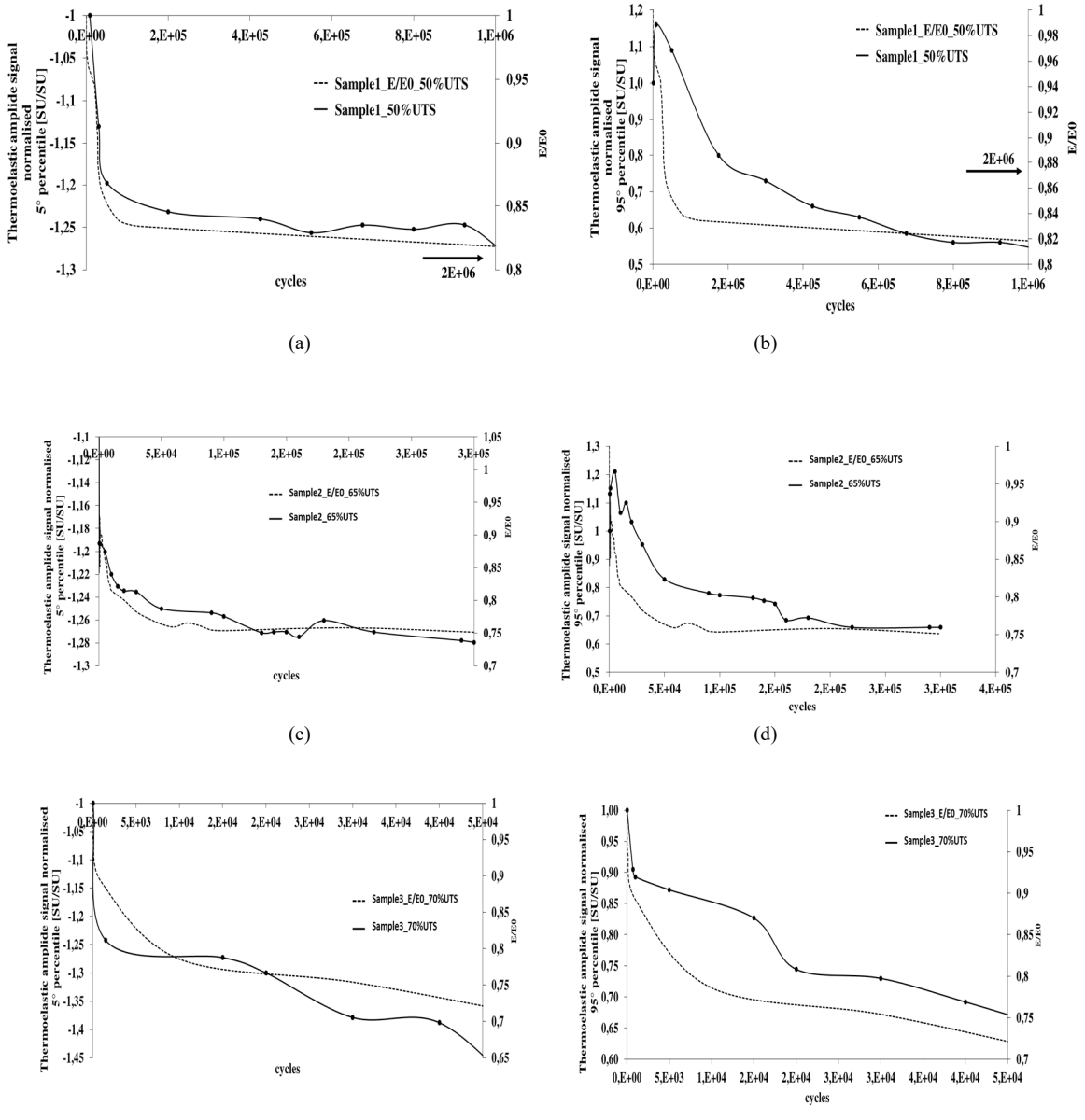

Fig. 5. Comparison between percentiles of thermoelastic signal variations: (a)(c)(e) 95° and (b)(d)(f) 5° percentile values at three stress levels of constant amplitude tests.

The most of these areas are detectable by early cycles whether the stress is high (Fig. 6c) or not (Fig. 6b).
Another remarkable effect is represented by the higher signal in the upper part of the sample which characterize all the test samples. This phenomenon is actually object of study, however is likely to be ascribed to the motion since the region is close to the moving grip of the loading frame.
The effect of motion causes the thermoelastic signal to ‘blur’. Observation of the affected area through the fatigue

loads shows motion becomes more significant as the stiffness reduces. This will be in depth investigated. This is especially true for those areas close to the aforementioned region however the area considered for the analysis refer to region where displacement are zero for most part of the test.
Hence, it is possible to conclude that the maps of thermoealstic signal allow the assessment in a qualitative way of the information about the early onset of material degradation and about the material carrying load capability.

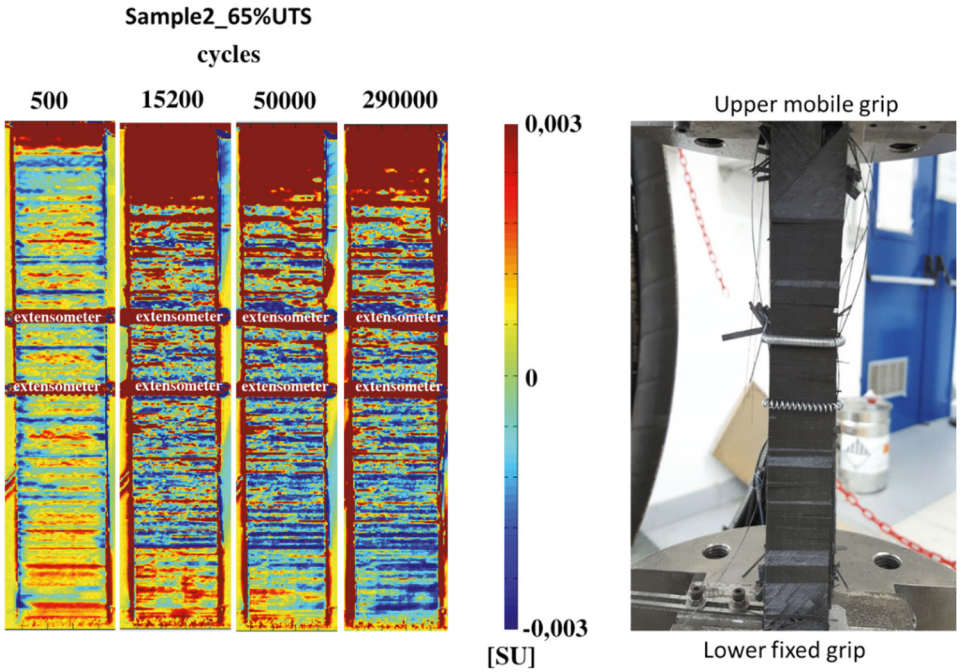

(a)

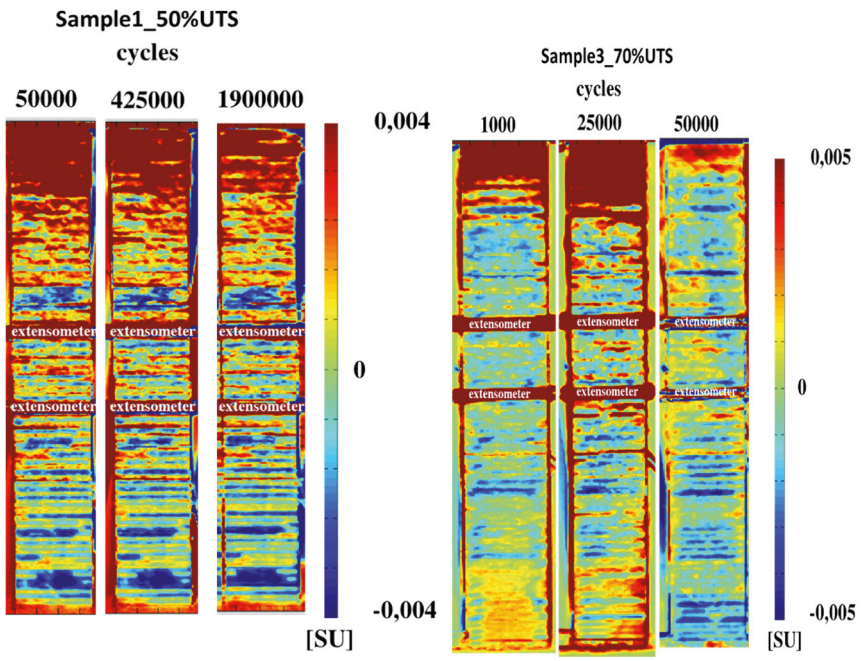

(b) (c)

Fig. 6. Maps of thermoelastic signal for (a) 50%UTS, (b) 65%UTS, (c)70%UTS tests.

Conclusions

In this work, a procedure has been proposed for studying the damage of composite materials obtained by automatic fiber placement by using thermographic metrics provided by infrared thermography.
The thermoelastic temperature signal was used as parameter to both assess the stress/strain redistribution in the material and the stiffness degradation. Three specimens of the reference SN curve performed were used for studying the thermoelastic maximum and minimum values compared with the data obtained by extensometer.
The samples were tested at respectively 50%UTS, 65%UTS, 70%UTS, of the material. The first value of the imposed stress corresponded to the runout at 2*10^6 cycles.
The analysis of thermoelastic signal metrics in terms of 95° percentile value, which in theory are related to the stress redistribution in the material showed particular trend characterised by an increase and immediate decreases followed a steady state. This involve in a several discrete equilibrium phases up to the failure. The thermoelastic variations (5° percentile of data) presented a trend which followed the those provided by mechanical data (E/E0) obtained by using an extensometer. In particular, the thermal parameter presented a severe decrease phase after the tests started, demonstrating the higher sensitivity with respect an extensometer to reflect any mechanical changes in the material.
Also, the analysis of the maps of thermoealstic parameter reported locally where and when the typical damage failure started. This demonstrates the capability of thermoelastic stress analysis to predict the failure area, then, the capability in performing also non destructing inspections.
The potential of the technique is related to the possibility of reducing testing time: from one thermographic sequence, different indexes can be extracted to study the fatigue behavior under different points of views. Furtherly, the proposed procedure could represent a useful tool for the monitoring of real and more complex components subjected to actual loading conditions.

Acknowledgements

The authors would like to thank Novotech Aerospace Advanced Technology S.R.L. for the manufacturing of the samples and Prof. Riccardo Nobile and Mr. Andrea Saponaro for the great support during the experimental activity performed in this work.

References

Bannister, M.K.,2004. Development and application of advanced textile composites. Proceedings of the Institution of Mechanical Engineers", Part L: Journal of Materials Design and Applications, 218, 253-260.
Palumbo, D., De Finis, R., Demelio, G.P., Galietti, U.,2016. A new rapid thermographic method to assess the fatigue limit in GFRP composites. Composite Part B, 103, 60-67.
Harris, B., 2003. Fatigue in composites, Cambridge: Woolhead Publishing Ltd.
Munoz, V., Valès, B., Perrin, M., Pastor, M.L., Welemane, H., Cantarel, A., 2016. Damage detection in CFRP by coupling acoustic emission and infrared thermography. Composites: Part B, 85, 68-75.
Goidescu, C., Welemane, H., Garnier, C., Fazzini, M., Brault, R., Péronnet, E., Mistou, S., 2013. Damage investigation in CFRP composites using full-field measurement technique: Combination of digital image stereo-correlation, infrared thermography and X-ray tomography. Composites: Part B, 48,95-105.
Naderi, M., Kahirdeh, A., Khonsari ,M.M., 2012. Dissipated thermal energy and damage evolution of Glass/Epoxy using infrared thermography and acoustic emission, Composites: Part B, 43, 1613-1620.
Kordatos, E.Z., Aggelis, D.G., Matikas, T.E., 2012. Monitoring mechanical damage in structural materials using complimentary NDE techniques based on thermography and acoustic emission", Composites: Part B, 43, 2676-2686.
Harwood, N., Cummings, W. Thermoelastic stress analysis, New York: National Engineering Laboratory; Adam Hilger, 1991.
Pittaresi, G., Patterson, E.A., 1999. A review of the general theory of thermoelastic stress analysis. Journal of Strains Analysis, 35, 35–39.
Wang, W.J., Dulieu-Barton, J.M., Li, Q., 2010.Assessment of Non-Adiabatic Behaviour in Thermoelastic Stress Analysis of Small Scale Components. Experimental Mechanics, 50,449-461.
Palumbo, D., Galietti, U., 2016. Data Correction for Thermoelastic Stress Analysis on Titanium Components. Experimental Mechanics, 56, 451-462.
Emery, T.R., Dulieu-Barton, J.K., 2010. Thermoelastic Stress Analysis of the damage mechanisms in composite materials. Composites: Part A, 41, 1729-1742.
Fruehmann, R.K., Dulieu-Barton, J.M., Quinn, S., 2010. Assessment of the fatigue damage evolution in woven composite materials using infra-red techniques. Composite Science and Technology, 70,937-946.
Denkenaa, B., Schmidtb, C., Weberb., P., 2016.Automated Fiber Placement Head for Manufacturing of Innovative Aerospace Stiffening Structures. Procedia Manufacturing 6, 96 – 104.

Aized, T., Shirinzadeh., B., 2011. Robotic fiber placement process analysis and optimization using response surface method. Int J Adv Manuf Technol, 55,393–404.

KozaczuK., K., 2016. Automated fiber placement systems overview. Transactions of the institute of aviation, 4 (245), 52-59.

Brüning, J., Denkena, B., Dittrich, M. A., Hocke, T., 2017. Machine Learning Approach for Optimization of Automated Fiber Placement Processes, Procedia CIRP, 66, 74 – 78.

Belhaj, M., Deleglise, M., et al, 2013. Dry fiber automated placement of carbon fibrous preforms", Composites: Part B 50, 107–111.

Zhao, P., Shirinzadeh., B., 2018. Multi-pass layup process for thermoplastic composites using robotic fiber placement. Robotics and Computer–Integrated Manufacturing 49, 277–284.

Belnoue, J. P.H. , Mesogitis., T. , 2017.Understanding the buckling behaviour of steered tows in Automated Dry FibrePlacement (ADFP) placement pre-preg laminates. Composites: Part A 102, 196–206.

Schmidt, C., Denkena B, et al. Thermal image-based monitoring for the automated fiber placement process. 10th CIRP Conference on Intelligent Computation in Manufacturing Engineering - CIRP ICME, 2016.

Lichtinger, R., Hörmann, P., Stelzl, D., Hinterhölzl. R., 2015. The effects of heat input on adjacent paths during Automated Fibre Placement". Composites: Part A 68, 387–397.

Krapez, C., Pacou D., Gardette, G.. "Lock-in thermography and fatigue limit of metals", ONERA, DMSE, BP 72, F-92322 CHÂTILLON-Cedex, France.

Montesano, J., Fawaz, Z., Bougherara, H., 2013. Use of infrared thermography to investigate the fatigue behavior of a carbon fiber reinforced polymner composite. Composite Structures, 97,76-83.

De Finis, R., Palumbo, D., Galietti, U., 2019. A multianalysis thermography-based approach for the fatigue and damage investigation of astm A182 F6NM steel at two stress ratios, Fatigue and Fracture of Engineering Materials and Structures, 42(1),267-283.

Palumbo, D., De Finis, R., Demelio, G.P., Galietti, U., 2017. Study of damage evolution in composite materials based on the Thermoelastic Phase Analysis (TPA) method. Composites Part B Engineering, 117, 49-60.

Pierron, F., Green, B., Wisnom, M.R.,2007. Full-field assessment of the damage process of laminated composite open-hole tensile specimens, Part I: methodology.Composites Part A 38, 2307–20.

Huanga, B., Pastor, M.L., Garnier, C., Gonga X.J., 2019. A new model for fatigue life prediction based on infrared thermography and degradation process for CFRP composite laminates. International Journal of Fatigue 120, 87–95.

Ospina Cadavid, M., Al-khudairi,O., Hadavinia,H., Goodwin, D., Liaghat, G.H., 2017. Experimental studies of stiffness degradation and dissipated energy in glass fibre reinforced polymer composite under fatigue loading. Polymers & Polymer Composites, 25 (6), 435-446.